Observation of Charge Asymmetry Dependence of Pion Elliptic Flow and the Possible Chiral Magnetic Wave in Heavy-Ion Collisions

(STAR Collaboration) Adamczyk, L.; ...; Planinić, Mirko; ...; Poljak, Nikola; ...; Zyzak, M.

Observation of Charge Asymmetry Dependence of Pion Elliptic Flow and the Possible Chiral Magnetic Wave in Heavy-Ion Collisions

L. Adamczyk,[1] J. K. Adkins,[20] G. Agakishiev,[18] M. M. Aggarwal,[30] Z. Ahammed,[47] I. Alekseev,[16] J. Alford,[19] A. Aparin,[18] D. Arkhipkin,[3] E. C. Aschenauer,[3] G. S. Averichev,[18] A. Banerjee,[47] R. Bellwied,[43] A. Bhasin,[17] A. K. Bhati,[30] P. Bhattarai,[42] J. Bielcik,[10] J. Bielcikova,[11] L. C. Bland,[3] I. G. Bordyuzhin,[16] J. Bouchet,[19] A. V. Brandin,[26] I. Bunzarov,[18] T. P. Burton,[3] J. Butterworth,[36] H. Caines,[51] M. Calderón de la Barca Sánchez,[5] J. M. Campbell,[28] D. Cebra,[5] M. C. Cervantes,[41] I. Chakaberia,[3] P. Chaloupka,[10] Z. Chang,[41] S. Chattopadhyay,[47] J. H. Chen,[39] X. Chen,[22] J. Cheng,[44] M. Cherney,[9] W. Christie,[3] G. Contin,[23] H. J. Crawford,[4] S. Das,[13] L. C. De Silva,[9] R. R. Debbe,[3] T. G. Dedovich,[18] J. Deng,[38] A. A. Derevschikov,[32] B. di Ruzza,[3] L. Didenko,[3] C. Dilks,[31] X. Dong,[23] J. L. Drachenberg,[46] J. E. Draper,[5] C. M. Du,[22] L. E. Dunkelberger,[6] J. C. Dunlop,[3] L. G. Efimov,[18] J. Engelage,[4] G. Eppley,[36] R. Esha,[6] O. Evdokimov,[8] O. Eyser,[3] R. Fatemi,[20] S. Fazio,[3] P. Federic,[11] J. Fedorisin,[18] Z. Feng,[7] P. Filip,[18] Y. Fisyak,[3] C. E. Flores,[5] L. Fulek,[1] C. A. Gagliardi,[41] D. Garand,[33] F. Geurts,[36] A. Gibson,[46] M. Girard,[48] L. Greiner,[23] D. Grosnick,[46] D. S. Gunarathne,[40] Y. Guo,[37] S. Gupta,[17] A. Gupta,[17] W. Guryn,[3] A. Hamad,[19] A. Hamed,[41] R. Haque,[27] J. W. Harris,[51] L. He,[33] S. Heppelmann,[3] S. Heppelmann,[31] A. Hirsch,[33] G. W. Hoffmann,[42] D. J. Hofman,[8] S. Horvat,[51] H. Z. Huang,[6] B. Huang,[8] X. Huang,[44] P. Huck,[7] T. J. Humanic,[28] G. Igo,[6] W. W. Jacobs,[15] H. Jang,[21] K. Jiang,[37] E. G. Judd,[4] S. Kabana,[19] D. Kalinkin,[16] K. Kang,[44] K. Kauder,[49] H. W. Ke,[3] D. Keane,[19] A. Kechechyan,[18] Z. H. Khan,[8] D. P. Kikola,[48] I. Kisel,[12] A. Kisiel,[48] D. D. Koetke,[46] T. Kollegger,[12] L. K. Kosarzewski,[48] L. Kotchenda,[26] A. F. Kraishan,[40] P. Kravtsov,[26] K. Krueger,[2] I. Kulakov,[12] L. Kumar,[30] R. A. Kycia,[29] M. A. C. Lamont,[3] J. M. Landgraf,[3] K. D. Landry,[6] J. Lauret,[3] A. Lebedev,[3] R. Lednicky,[18] J. H. Lee,[3] W. Li,[39] Y. Li,[44] C. Li,[37] N. Li,[7] Z. M. Li,[7] X. Li,[40] X. Li,[3] M. A. Lisa,[28] F. Liu,[7] T. Ljubicic,[3] W. J. Llope,[49] M. Lomnitz,[19] R. S. Longacre,[3] X. Luo,[7] L. Ma,[39] R. Ma,[3] Y. G. Ma,[39] G. L. Ma,[39] N. Magdy,[50] R. Majka,[51] A. Manion,[23] S. Margetis,[19] C. Markert,[42] H. Masui,[23] H. S. Matis,[23] D. McDonald,[43] K. Meehan,[5] N. G. Minaev,[32] S. Mioduszewski,[41] B. Mohanty,[27] M. M. Mondal,[41] D. A. Morozov,[32] M. K. Mustafa,[23] B. K. Nandi,[14] Md. Nasim,[6] T. K. Nayak,[47] G. Nigmatkulov,[26] L. V. Nogach,[32] S. Y. Noh,[21] J. Novak,[25] S. B. Nurushev,[32] G. Odyniec,[23] A. Ogawa,[3] K. Oh,[34] V. Okorokov,[26] D. L. Olvitt, Jr.,[40] B. S. Page,[3] R. Pak,[3] Y. X. Pan,[6] Y. Pandit,[8] Y. Panebratsev,[18] B. Pawlik,[29] H. Pei,[7] C. Perkins,[4] A. Peterson,[28] P. Pile,[3] M. Planinic,[52] J. Pluta,[48] N. Poljak,[52] K. Poniatowska,[48] J. Porter,[23] M. Posik,[40] A. M. Poskanzer,[23] N. K. Pruthi,[30] J. Putschke,[49] H. Qiu,[23] A. Quintero,[19] S. Ramachandran,[20] S. Raniwala,[35] R. Raniwala,[35] R. L. Ray,[42] H. G. Ritter,[23] J. B. Roberts,[36] O. V. Rogachevskiy,[18] J. L. Romero,[5] A. Roy,[47] L. Ruan,[3] J. Rusnak,[11] O. Rusnakova,[10] N. R. Sahoo,[41] P. K. Sahu,[13] I. Sakrejda,[23] S. Salur,[23] J. Sandweiss,[51] A. Sarkar,[14] J. Schambach,[42] R. P. Scharenberg,[33] A. M. Schmah,[23] W. B. Schmidke,[3] N. Schmitz,[24] J. Seger,[9] P. Seyboth,[24] N. Shah,[6] E. Shahaliev,[18] P. V. Shanmuganathan,[19] M. Shao,[37] B. Sharma,[30] M. K. Sharma,[17] W. Q. Shen,[39] S. S. Shi,[7] Q. Y. Shou,[39] E. P. Sichtermann,[23] R. Sikora,[1] M. Simko,[11] M. J. Skoby,[15] D. Smirnov,[3] N. Smirnov,[51] L. Song,[43] P. Sorensen,[3] H. M. Spinka,[2] B. Srivastava,[33] T. D. S. Stanislaus,[46] M. Stepanov,[33] R. Stock,[12] M. Strikhanov,[26] B. Stringfellow,[33] M. Sumbera,[11] B. J. Summa,[31] X. Sun,[23] X. M. Sun,[7] Z. Sun,[22] Y. Sun,[37] B. Surrow,[40] D. N. Svirida,[16] M. A. Szelezniak,[23] Z. Tang,[37] A. H. Tang,[3] T. Tarnowsky,[25] A. N. Tawfik,[50] J. H. Thomas,[23] A. R. Timmins,[43] D. Tlusty,[11] M. Tokarev,[18] S. Trentalange,[6] R. E. Tribble,[41] P. Tribedy,[47] S. K. Tripathy,[13] B. A. Trzeciak,[10] O. D. Tsai,[6] T. Ullrich,[3] D. G. Underwood,[2] I. Upsal,[28] G. Van Buren,[3] G. van Nieuwenhuizen,[3] M. Vandenbroucke,[40] R. Varma,[14] A. N. Vasiliev,[32] R. Vertesi,[11] F. Videbaek,[3] Y. P. Viyogi,[47] S. Vokal,[18] S. A. Voloshin,[49] A. Vossen,[15] F. Wang,[33] Y. Wang,[44] H. Wang,[3] J. S. Wang,[22] Y. Wang,[7] G. Wang,[6] G. Webb,[3] J. C. Webb,[3] L. Wen,[6] G. D. Westfall,[25] H. Wieman,[23] S. W. Wissink,[15] R. Witt,[45] Y. F. Wu,[7] Z. Xiao,[44] W. Xie,[33] K. Xin,[36] Y. F. Xu,[39] N. Xu,[23] Z. Xu,[3] Q. H. Xu,[38] H. Xu,[22] Y. Yang,[7] Y. Yang,[22] C. Yang,[37] S. Yang,[37] Q. Yang,[37] Z. Ye,[8] P. Yepes,[36] L. Yi,[33] K. Yip,[3] I.-K. Yoo,[34] N. Yu,[7] H. Zbroszczyk,[48] W. Zha,[37] X. P. Zhang,[44] J. B. Zhang,[7] J. Zhang,[22] Z. Zhang,[39] S. Zhang,[39] Y. Zhang,[37] J. L. Zhang,[38] F. Zhao,[6] J. Zhao,[7] C. Zhong,[39] L. Zhou,[37] X. Zhu,[44] Y. Zoulkarneeva,[18] and M. Zyzak[12]

(STAR Collaboration)

[1]*AGH University of Science and Technology, Cracow 30-059, Poland*
[2]*Argonne National Laboratory, Argonne, Illinois 60439, USA*
[3]*Brookhaven National Laboratory, Upton, New York 11973, USA*
[4]*University of California, Berkeley, California 94720, USA*
[5]*University of California, Davis, California 95616, USA*

[6]University of California, Los Angeles, California 90095, USA
[7]Central China Normal University (HZNU), Wuhan 430079, China
[8]University of Illinois at Chicago, Chicago, Illinois 60607, USA
[9]Creighton University, Omaha, Nebraska 68178, USA
[10]Czech Technical University in Prague, FNSPE, Prague 115 19, Czech Republic
[11]Nuclear Physics Institute AS CR, 250 68 Řež/Prague, Czech Republic
[12]Frankfurt Institute for Advanced Studies FIAS, Frankfurt 60438, Germany
[13]Institute of Physics, Bhubaneswar 751005, India
[14]Indian Institute of Technology, Mumbai 400076, India
[15]Indiana University, Bloomington, Indiana 47408, USA
[16]Alikhanov Institute for Theoretical and Experimental Physics, Moscow 117218, Russia
[17]University of Jammu, Jammu 180001, India
[18]Joint Institute for Nuclear Research, Dubna 141 980, Russia
[19]Kent State University, Kent, Ohio 44242, USA
[20]University of Kentucky, Lexington, Kentucky 40506-0055, USA
[21]Korea Institute of Science and Technology Information, Daejeon 305-701, Korea
[22]Institute of Modern Physics, Lanzhou 730000, China
[23]Lawrence Berkeley National Laboratory, Berkeley, California 94720, USA
[24]Max-Planck-Institut fur Physik, Munich 80805, Germany
[25]Michigan State University, East Lansing, Michigan 48824, USA
[26]Moscow Engineering Physics Institute, Moscow 115409, Russia
[27]National Institute of Science Education and Research, Bhubaneswar 751005, India
[28]The Ohio State University, Columbus, Ohio 43210, USA
[29]Institute of Nuclear Physics PAN, Cracow 31-342, Poland
[30]Panjab University, Chandigarh 160014, India
[31]Pennsylvania State University, University Park, Pennsylvania 16802, USA
[32]Institute of High Energy Physics, Protvino 142281, Russia
[33]Purdue University, West Lafayette, Indiana 47907, USA
[34]Pusan National University, Pusan 609735, Republic of Korea
[35]University of Rajasthan, Jaipur 302004, India
[36]Rice University, Houston, Texas 77251, USA
[37]University of Science and Technology of China, Hefei 230026, China
[38]Shandong University, Jinan, Shandong 250100, China
[39]Shanghai Institute of Applied Physics, Shanghai 201800, China
[40]Temple University, Philadelphia, Pennsylvania 19122, USA
[41]Texas A&M University, College Station, Texas 77843, USA
[42]University of Texas, Austin, Texas 78712, USA
[43]University of Houston, Houston, Texas 77204, USA
[44]Tsinghua University, Beijing 100084, China
[45]United States Naval Academy, Annapolis, Maryland 21402, USA
[46]Valparaiso University, Valparaiso, Indiana 46383, USA
[47]Variable Energy Cyclotron Centre, Kolkata 700064, India
[48]Warsaw University of Technology, Warsaw 00-661, Poland
[49]Wayne State University, Detroit, Michigan 48201, USA
[50]World Laboratory for Cosmology and Particle Physics (WLCAPP), Cairo 11571, Egypt
[51]Yale University, New Haven, Connecticut 06520, USA
[52]University of Zagreb, Zagreb HR-10002, Croatia

(Received 10 April 2015; published 26 June 2015)

We present measurements of π^- and π^+ elliptic flow, v_2, at midrapidity in Au + Au collisions at $\sqrt{s_{\rm NN}} = 200$, 62.4, 39, 27, 19.6, 11.5, and 7.7 GeV, as a function of event-by-event charge asymmetry, $A_{\rm ch}$, based on data from the STAR experiment at RHIC. We find that π^- (π^+) elliptic flow linearly increases (decreases) with charge asymmetry for most centrality bins at $\sqrt{s_{\rm NN}} = 27$ GeV and higher. At $\sqrt{s_{\rm NN}} = 200$ GeV, the slope of the difference of v_2 between π^- and π^+ as a function of $A_{\rm ch}$ exhibits a centrality dependence, which is qualitatively similar to calculations that incorporate a chiral magnetic wave effect. Similar centrality dependence is also observed at lower energies.

DOI: 10.1103/PhysRevLett.114.252302 PACS numbers: 25.75.-q, 25.75.Ld

In heavy-ion collisions at the Relativistic Heavy Ion Collider (RHIC) and the Large Hadron Collider (LHC), energetic spectator protons produce a strong magnetic field reaching $eB_y \approx m_\pi^2$ [1], or $\sim 3 \times 10^{14}$ T. The interplay between the magnetic field and the quark-gluon matter created in these collisions might result in two phenomena: the chiral magnetic effect (CME) and the chiral separation effect (CSE). The CME is the phenomenon of electric charge separation along the axis of the magnetic field in the presence of a finite axial chemical potential [1–5]. The STAR [6–9] and PHENIX [10,11] Collaborations at the RHIC and the ALICE Collaboration at the LHC [12] have reported experimental observations of charge separation fluctuations, possibly providing evidence for the CME. This interpretation is still under discussion (see e.g. [13–15] and references therein). The CSE refers to the separation of chiral charge, which characterizes left or right handedness, along the axis of the magnetic field in the presence of the finite density of electric charge [16,17]. In this Letter, we report the results from a search for these effects using a new approach.

In a chirally symmetric phase, the CME and CSE can form a collective excitation, the chiral magnetic wave (CMW). It is a propagation of chiral charge density in a long wavelength hydrodynamic mode [18–20]. The CMW, which requires chiral symmetry restoration, manifests itself in a finite electric quadrupole moment of the collision system, where the "poles" ("equator") of the collision system acquire additional positive (negative) charge [18]. This effect, if present, will increase (decrease) the elliptic flow of negative (positive) particles. Elliptic flow refers to an azimuthally anisotropic collective motion of soft (low momentum) particles. It is characterized by a second-order harmonic in a particle's azimuthal distribution, ϕ, with respect to the reaction plane azimuthal angle, $\Psi_{\rm RP}$, which is determined by the impact parameter and the beam direction,

$$v_2 = \langle \cos[2(\phi - \Psi_{\rm RP})] \rangle. \quad (1)$$

The CMW is theoretically expected to modify the elliptic flow of charged particles, e.g. pions, on top of the baseline $v_2^{\rm base}(\pi^\pm)$ [18]

$$v_2(\pi^\pm) = v_2^{\rm base}(\pi^\pm) \mp \frac{r}{2} A_{\rm ch}, \quad (2)$$

where r is the quadrupole moment normalized by the net charge density and $A_{\rm ch} = (N_+ - N_-)/(N_+ + N_-)$ is the charge asymmetry of the collision system. As the colliding nuclei are positively charged, the average charge asymmetry $\langle A_{\rm ch} \rangle$ is always positive. Thus, the $A_{\rm ch}$-integrated v_2 of π^- (π^+) should be above (below) the baseline because of the CMW. However, the $v_2^{\rm base}$ may be different between π^+ and π^- because of several other possible physical mechanisms [21–24]. It is preferable to study CMW via the $A_{\rm ch}$ dependence of the pion v_2 other than $A_{\rm ch}$-integrated v_2.

This Letter reports the $A_{\rm ch}$-differential measurements of the pion v_2, based on Au+Au samples of 2×10^8 events at 200 GeV from RHIC year 2010, 6×10^7 at 62.4 GeV (2010), 10^8 at 39 GeV (2010), 4.6×10^7 at 27 GeV (2011), 2×10^7 at 19.6 GeV (2011), 1×10^7 for 11.5 (2010), and 4×10^6 for 7.7 GeV (2010). All events were obtained with a minimum-bias trigger which selects all particle-producing collisions, regardless of the extent of overlap of the incident nuclei [25]. Charged particle tracks with pseudorapidity $|\eta| < 1$ were reconstructed in the STAR time projection chamber (TPC) [26]. The number of charged particles within $|\eta| < 0.5$ is used to define the centrality. The centrality definitions and track quality cuts are the same as those used in Ref. [27], unless otherwise specified. Only events within 40 cm (50 cm for 11.5 GeV and 70 cm for 7.7 GeV) of the center of the detector center along the beam line direction are selected. To suppress events from collisions with the beam pipe (radius = 3.95 cm), a cut on the radial position of the reconstructed primary vertex within 2 cm was applied. A cut on the distance of the closest approach to the primary vertex (DCA< 1 cm) was applied to all tracks to suppress contributions from weak decays and/or secondary interactions.

The observed $A_{\rm ch}$ was determined from the measured charged particles with transverse momentum $p_T > 0.15$ GeV/c and $|\eta| < 1$; protons and antiprotons with $p_T < 0.4$ GeV/c were excluded to reject background protons from the nuclear interactions of pions with inner detector materials. Figure 1(a) shows an example of the observed $A_{\rm ch}$ distribution, which was divided into five samples roughly containing equal numbers of events, as indicated by the dashed lines. Figure 1(b) shows the relationship between the observed $A_{\rm ch}$ and the $A_{\rm ch}$ from the HIJING event generator [28], where the same cuts as used in data were applied to calculate $A_{\rm ch}$. The relationship is linear. To select pions with high purity, we eliminate charged particles more than 2σ away from the expected energy loss of pions in the TPC. For energies less than or

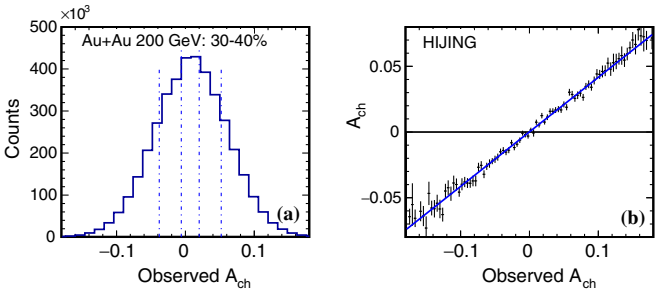

FIG. 1 (color online). (a) Distribution of observed charge asymmetry from STAR data and, (b) the relationship between the observed charge asymmetry and the charge asymmetry from HIJING generated events, for 30%–40% central Au + Au collisions at 200 GeV. In this centrality, the mean charge asymmetry $\langle A_{\rm ch} \rangle$ of HIJING events is about 0.004. The errors are statistical only.

equal to 62.4 GeV, elliptic flow measurements were carried out with the $v_2\{\eta\text{sub}\}$ approach [29], where two subevent planes register charged particles with $\eta > 0.3$ and $\eta < -0.3$, respectively. Pions at positive (negative) η are then correlated with the subevent plane at negative (positive) η to calculate v_2. The η gap of 0.3 unit suppresses several short-range correlations such as the Bose-Einstein interference and the Coulomb final-state interactions [30]. There are correlations that are unrelated to the reaction plane that are not suppressed by the η gap, e.g. those due to back-to-back jets. These are largely canceled in the v_2 difference between π^- and π^+. For 200 GeV, the two-particle cumulant method $v_2\{2\}$ [30,31] was employed, which was consistent with $v_2\{\eta\text{sub}\}$, and allowed the comparison with the $v_2\{4\}$ method discussed later in this Letter. The same η gap was also used in the $v_2\{2\}$ analysis. To focus on the soft physics regime, only pions with $0.15 < p_T < 0.5$ GeV/c were used to calculate the p_T-integrated v_2, and this p_T range covers 65%–70% of all the produced pions. The calculation of the p_T-integrated v_2 was corrected with the p_T-dependent tracking efficiency for pions.

Taking Au + Au 200 GeV collisions in the 30%–40% centrality range as an example, the pion v_2 is shown as a function of the observed A_{ch} in Fig. 2(a). The $\pi^- v_2$ increases with increasing observed A_{ch} while the $\pi^+ v_2$ decreases with a similar magnitude of the slope. After applying the tracking efficiency to A_{ch}, the v_2 difference between π^- and π^+ has been fitted with a straight line as shown in Fig. 2(b). The slope parameter r from Eq. (2) is positive and qualitatively consistent with the expectations of the CMW picture. The fit function is nonzero at the average charge asymmetry $\langle A_{\text{ch}} \rangle$, which is a small positive number in the case of Au + Au collisions. This indicates the A_{ch}-integrated v_2 for π^- and π^+ are different, which was observed in Ref. [32]. We follow the same procedure as above to extract the slope parameter r for all centrality bins at 200 GeV. The results are shown in Fig. 3, together with simulations using the UrQMD event generator [33] and with the theoretical calculations with CMW [34] with different duration times of the magnetic field. For most data points, the slopes are positive and reach a maximum in midcentral or midperipheral collisions, a feature also seen in the theoretical calculations of the CMW. The gray bands in Fig. 3 include three types of systematic errors: the DCA cut for pion tracks was tightened to 0.5 cm, to study the contribution from weak decays, which dominates the systematic errors; the tracking efficiency for charged particles was varied by relative 5%, to determine the uncertainty of A_{ch}; and the p_T range of particles involved in the event plane determination was shrunk from $[0.15, 2]$ GeV/c to $[0.7, 2]$ GeV/c, to further suppress short-range correlations. The A_{ch} bin center may not accurately reflect the true center of each A_{ch} bin in Fig. 2, as the v_2 measurements are effectively weighted by the number of particles of interest. Such an uncertainty on r has been estimated to be negligible for most centrality bins, except for the most peripheral collisions, where this systematic error is still much smaller than the statistical error.

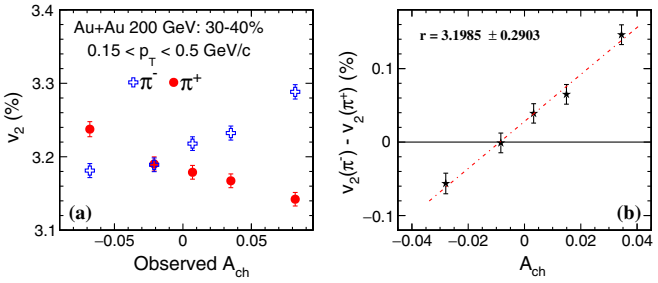

FIG. 2 (color online). (a) Pion $v_2\{2\}$ as a function of observed charge asymmetry and (b) v_2 difference between π^- and π^+ as a function of charge asymmetry with the tracking efficiency correction, for 30%–40% central Au + Au collisions at 200 GeV. The errors are statistical only.

To further study the charge-dependent contribution from jets and/or resonance decays, we separated positive and negative particles in each subevent to form positively (negatively) charged subevents. Then each π^+ (π^-) is only correlated with the positive (negative) subevent in the opposite hemisphere. The slope parameters thus obtained are statistically consistent with the previous results though with larger uncertainties.

The event plane reconstructed with particles recorded in the TPC approximates the participant plane; the measured v_2 are not the mean values, but closer to the root-mean-square values [35]. Another method, $v_2\{4\}$ [36] is supposed to better represent the v_2 measurement with respect

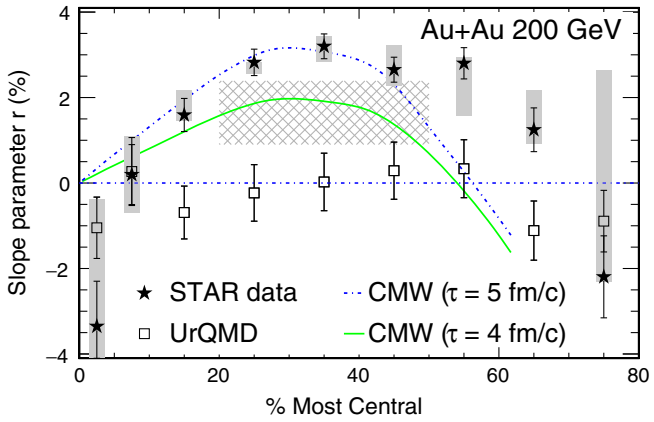

FIG. 3 (color online). The slope parameter, r, as a function of centrality for Au + Au collisions at 200 GeV. Also shown is the UrQMD [33] simulation, and the calculations with CMW [34] with different duration times. The grey bands include the systematic errors due to the DCA cut, the tracking efficiency, and the p_T range of particles involved in the event plane determination. The cross-hatched band indicates the STAR measurement with the $v_2\{4\}$ method and the height of this band shows only the statistical error.

to the reaction plane. For 20%–50% Au + Au collisions at 200 GeV, the slope parameter obtained with $v_2\{4\}$ is illustrated with the cross-hatched band in Fig. 3, which is systematically lower than the $v_2\{2\}$ results, but still has a finite positive value with a larger statistical error.

Since the prediction of the consequence of CMW on v_2 [18,19], this subject has recently drawn increasing attention from theorists [34,37–42]. It was pointed out in Ref. [42] that local charge conservation at freeze-out, when convoluted with the characteristic shape of $v_2(p_T)$ and $v_2(\eta)$, may provide a qualitative explanation for the finite v_2 slope we observe. Such an effect depends on the strength of the $A_{\rm ch}$ dependence on the mean p_T and the η dependence of v_2. However, our measurements were carried out in a narrow p_T range ($[0.15, 0.5]$ GeV/c) and with a $\langle p_T\rangle(A_{\rm ch})$ variation of 0.1% at most. Furthermore, the measured η dependence of v_2 is only half as strong as that used in Ref. [42]. We estimate the contribution of this mechanism to be smaller than the measurement by an order of magnitude.

To check if the observed slope parameters come from conventional physics, such as Coulomb interactions, or from a bias due to the analysis approach, we carried out the same analysis in Monte Carlo events from UrQMD. As shown in Fig. 3, the slopes extracted from UrQMD events of 200 GeV Au + Au collisions are consistent with zero for 10%–60% centrality collisions, where the signal is prominent in the data. Similarly, the AMPT event generator [43,44] also produces events with slopes r consistent with zero. With the AMPT model, we also studied the weak decay contribution to the slope, which was negligible. On the other hand, the CMW calculations [18] demonstrate a similar centrality dependence of the slope parameter. Recently, a more realistic implementation of the CMW [40] suggested that the CMW contribution to r is sizable, and the centrality dependence of r is similar to the data. In these theoretical calculations such centrality dependence mainly results from the centrality dependence of the magnetic field and the system volume. Quantitative comparisons between data and theory require further work on both sides to match the kinematic regions used in the analyses. For example, the measured $A_{\rm ch}$ only represents the charge asymmetry of a slice ($|\eta| < 1$) of an event, instead of that of the whole collision system. We expect these two values of $A_{\rm ch}$ to be proportional to each other, but the determination of the ratio will be model dependent. In addition to the UrQMD and AMPT simulation studies which reveal no trivial correlation between $A_{\rm ch}$ and pion v_2, tests were performed using the experimental data. For example, $A_{\rm ch}$ and the pion v_2 were calculated in two kinematically separated regions, i.e., different rapidity bins. In such cases, the slope parameters decrease but remain significant and positive. This may reflect the local nature of the $A_{\rm ch}$ dependence of v_2, but additional theoretical development is necessary.

Figure 4 shows a similar trend in the centrality dependence of the slope parameter for all the beam energies except 11.5 and 7.7 GeV, where the slopes are consistent with zero with large statistical uncertainties. It was argued [21] that at lower beam energies the $A_{\rm ch}$-integrated v_2 difference between particles and antiparticles can be explained by the effect of quark transport from the projectile nucleons to midrapidity, assuming that the v_2 of transported quarks is larger than that of produced ones. The same model, however, when used to study $v_2(\pi^-) - v_2(\pi^+)$ as a function of $A_{\rm ch}$, suggested a negative slope [45], which is contradicted by the data.

The mean field potentials from the hadronic phase [22] and the partonic phase [24] also qualitatively explain the $A_{\rm ch}$-integrated v_2 difference between particles and antiparticles, especially at lower beam energies. In general, the mean field potential is expected to be positively correlated with $A_{\rm ch}$ and thus may explain the trends in those data, but no conclusive statement can be made here due to the lack of specific predictions. This effect may be tested in the future by studying the $K^{\pm}v_2$ slopes, whose v_2 ordering is opposite to that of $\pi^{\pm}$.

In summary, pion v_2 exhibits a linear dependence on $A_{\rm ch}$, with positive (negative) slopes for π^- (π^+). The $v_2(\pi^-) - v_2(\pi^+)$ increases as a function of $A_{\rm ch}$, qualitatively

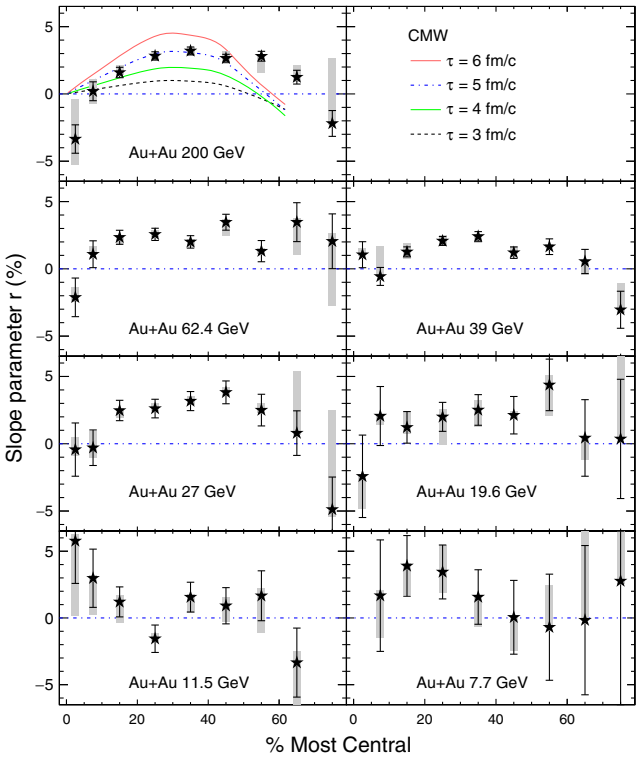

FIG. 4 (color online). The slope parameter r as a function of centrality for all the collision energies under study. For comparison, we also show the calculations with CMW [34] with different duration times. The grey bands carry the same meaning as those in Fig. 3.

reproducing the expectation from the CMW model. The slope r of $v_2(A_{\mathrm{ch}})$ difference between π^- and π^+ has been studied as a function of centrality, and we observe a dependence also similar to the calculation based on the CMW model. The slope parameter r remains significantly positive for 10%–60% centrality Au + Au collisions at $\sqrt{s_{\mathrm{NN}}} = 27$–200 GeV, and displays no obvious trend of the beam energy dependence with the current statistics. None of the conventional models discussed, as currently implemented, can explain our observations.

We thank the RHIC Operations Group and RCF at BNL, the NERSC Center at LBNL, the KISTI Center in Korea, and the Open Science Grid consortium for providing resources and support. This work was supported in part by the Office of Nuclear Physics within the U.S. DOE Office of Science, the U.S. NSF, the Ministry of Education and Science of the Russian Federation, NNSFC, CAS, MoST (973 Program No. 2014CB845400) and MoE of China, the Korean Research Foundation, GA and MSMT of the Czech Republic, FIAS of Germany, DAE, DST, and UGC of India, the National Science Center of Poland, National Research Foundation, the Ministry of Science, Education and Sports of the Republic of Croatia, and RosAtom of Russia.

[1] D. E. Kharzeev, L. D. McLerran, and H. J. Warringa, Nucl. Phys. **A803**, 227 (2008).
[2] D. Kharzeev, Phys. Lett. B **633**, 260 (2006).
[3] D. Kharzeev and A. Zhitnitsky, Nucl. Phys. **A797**, 67 (2007).
[4] K. Fukushima, D. E. Kharzeev, and H. J. Warringa, Phys. Rev. D **78**, 074033 (2008).
[5] D. E. Kharzeev, Ann. Phys. (Amsterdam) **325**, 205 (2010).
[6] B. I. Abelev *et al.* (STAR Collaboration), Phys. Rev. Lett. **103**, 251601 (2009).
[7] B. I. Abelev *et al.* (STAR Collaboration), Phys. Rev. C **81**, 054908 (2010).
[8] L. Adamczyk *et al.* (STAR Collaboration), Phys. Rev. C **88**, 064911 (2013).
[9] L. Adamczyk *et al.* (STAR Collaboration), Phys. Rev. Lett. **113**, 052302 (2014).
[10] N. N. Ajitanand, S. Esumi, and R. A. Lacey (PHENIX Collaboration), in *Proceedings of the RBRC Workshops* (Upton, New York, 2010), Vol. 96.
[11] N. N. Ajitanand, R. A. Lacey, A. Taranenko, and J. M. Alexander, Phys. Rev. C **83**, 011901 (2011).
[12] B. I. Abelev *et al.* (ALICE Collaboration), Phys. Rev. Lett. **110**, 012301 (2013).
[13] A. Bzdak, V. Koch, and J. Liao, Phys. Rev. C **81**, 031901 (2010); J. Liao, V. Koch, and A. Bzdak, Phys. Rev. C **82**, 054902 (2010).
[14] D. E. Kharzeev and D. T. Son, Phys. Rev. Lett. **106**, 062301 (2011).
[15] L. Adamczyk *et al.* (STAR Collaboration), Phys. Rev. C **89**, 044908 (2014).
[16] D. T. Son and A. R. Zhitnitsky, Phys. Rev. D **70**, 074018 (2004).
[17] M. A. Metlitski and A. R. Zhitnitsky, Phys. Rev. D **72**, 045011 (2005).
[18] Y. Burnier, D. E. Kharzeev, J. Liao, and H.-U. Yee, Phys. Rev. Lett. **107**, 052303 (2011).
[19] G. M. Newman, J. High Energy Phys. 01 (2006) 158.
[20] E. V. Gorbar, V. A. Miransky, and I. A. Shovkovy, Phys. Rev. D **83**, 085003 (2011).
[21] J. C. Dunlop, M. A. Lisa, and P. Sorensen, Phys. Rev. C **84**, 044914 (2011).
[22] J. Xu, L.-W. Chen, C. M. Ko, and Z.-W. Lin, Phys. Rev. C **85**, 041901 (2012).
[23] J. Steinheimer, V. Koch, and M. Bleicher, Phys. Rev. C **86**, 044903 (2012).
[24] C. M. Ko, T. Song, F. Li, V. Greco, and S. Plumari, Nucl. Phys. **A928**, 234 (2014).
[25] F. Bieser *et al.*, Nucl. Instrum. Methods Phys. Res., Sect. A **499**, 766 (2003).
[26] M. Anderson *et al.*, Nucl. Instrum. Methods Phys. Res., Sect. A **499**, 659 (2003).
[27] L. Adamczyk *et al.* (STAR Collaboration), Phys. Rev. C **86**, 054908 (2012).
[28] M. Gyulassy and X.-N. Wang, Comput. Phys. Commun. **83**, 307 (1994); X. N. Wang and M. Gyulassy, Phys. Rev. D **44**, 3501 (1991).
[29] A. M. Poskanzer and S. A. Voloshin, Phys. Rev. C **58**, 1671 (1998).
[30] J. Adams *et al.* (STAR Collaboration), Phys. Rev. C **72**, 014904 (2005).
[31] S. Voloshin and Y. Zhang, Z. Phys. C **70**, 665 (1996).
[32] L. Adamczyk *et al.* (STAR Collaboration), Phys. Rev. Lett. **110**, 142301 (2013).
[33] S. A. Bass *et al.*, Prog. Part. Nucl. Phys. **41**, 255 (1998); M. Bleicher *et al.*, J. Phys. G **25**, 1859 (1999).
[34] Y. Burnier, D. E. Kharzeev, J. Liao, and H.-U. Yee, arXiv:1208.2537; Y. Burnier (private communication).
[35] J.-Y. Ollitrault, A. M. Poskanzer, and S. A. Voloshin, Phys. Rev. C **80**, 014904 (2009).
[36] N. Borghini, P. M. Dinh, and J.-Y. Ollitrault, Phys. Rev. C **63**, 054906 (2001); A. Bilandzic, R. Snellings, and S. A. Voloshin, Phys. Rev. C **83**, 044913 (2011); S. A. Voloshin, A. M. Poskanzer, A. Tang, and G. Wang, Phys. Lett. B **659**, 537 (2008).
[37] M. Stephanov and H.-U. Yee, Phys. Rev. C **88**, 014908 (2013).
[38] M. Hongo, Y. Hirono, and T. Hirano, arXiv:1309.2823.
[39] S. F. Taghavi and U. A. Wiedemann, Phys. Rev. C **91**, 024902 (2015).
[40] H.-U. Yee and Y. Yin, Phys. Rev. C **89**, 044909 (2014).
[41] J. Bloczynski, X.-G. Huang, X. Zhang, and J. Liao, Phys. Lett. B **718**, 1529 (2013).
[42] A. Bzdak and P. Bozek, Phys. Lett. B **726**, 239 (2013).
[43] Z.-W. Lin and C. M. Ko, Phys. Rev. C **65**, 034904 (2002); L.-W. Chen and C. M. Ko, J. Phys. G **31**, S49 (2005).
[44] G.-L. Ma, Phys. Lett. B **735**, 383 (2014).
[45] J. M. Campbell and M. A. Lisa, J. Phys. Conf. Ser. **446**, 012014 (2013).